PERGAMON

Microelectronics Reliability 39 (1999) 107–112

MICROELECTRONICS RELIABILITY

Ball grid array reliability assessment for aerospace applications

R. Ghaffarian [a,*], N.P. Kim [b]

[a] *Jet Propulsion Laboratory, California Institute of Technology, Pasadena, CA 91109, USA*
[b] *Boeing Defense and Space Group, Seattle, Washington, USA*

Received 20 April 1998; received in revised form 10 August 1998

Abstract

Reliability of ball grid arrays (BGAs) was evaluated with special emphasis on space applications. This work was performed as part of a consortium led by the Jet Propulsion Laboratory (JPL) to help build the infrastructure necessary for implementing this technology. Nearly 200 test vehicles, each with four package types, were assembled and tested using an experiment design. The most critical variables incorporated in this experiment were package type, board material, surface finish, solder volume, and environmental condition. The packages used for this experiment were commercially available packages with over 250 I/Os including both plastic and ceramic BGA packages.

The test vehicles were subjected to thermal and dynamic environments representative of aerospace applications. Two different thermal cycling conditions were used, the JPL cycle ranged from −30°C to 100°C and the Boeing cycle ranged from −55°C to 125°C. The test vehicles were monitored continuously to detect electrical failure and their failure mechanisms were characterized. They were removed periodically for optical inspection, scanning electron microscopy (SEM) evaluation, and cross-sectioning for crack propagation mapping. Data collected from both facilities were analyzed and fitted to distributions using the Weibull distribution and Coffin–Manson relationships for failure projection. This paper will describe experiment results as well as those analyses.

1. Introduction

BGA is an important technology for utilizing higher pin counts, without the attendant handling and processing problems of the peripheral array packages. They are also robust in processing because of their higher pitch (0.050 in. typical), better lead rigidity, and self-alignment characteristics during reflow processing.

BGAs solder joints cannot be inspected and reworked using conventional methods and are not well characterized for multiple double sided assembly processing methods. In ultra low and low volume SMT assembly applications, e.g. space and defense, the ability to inspect the solder joints visually has been standard and has been a key factor for providing confidence in solder joint reliability.

To address many common quality and reliability issues of BGAs, JPL organized a consortium with 16 members in early 1995 [1]. The diverse membership included military, commercial, academia and infrastructure sectors which permitted a concurrent engineering approach for resolving many challenging technical issues. This paper will present the most current experiment results for the test vehicles assembled under the direction of this consortium. The board level thermal cycling data for ceramic packages with 625 I/O, plastic packages with 313 and 352 I/Os will be presented. Analysis and testing of other assemblies is

* Corresponding author. Tel.: 001 818 354 2059; Fax: 001 818 393 5245; E-mail:reza.ghaffarian@jpl.nasa.gov.

0026-2714/99/$ - see front matter
PII: S0026-2714(98)00185-1

Table 1
Package characteristics

Part type	I/O	Materials configurations	Size (mm sq)	Wiring	Pitch	Selected die size
"PBGA 300"	352	Plastic/peripheral/SUPER BGA	35	Daisy	1.27	13.3
"PBGA 300"	352	Plastic/peripheral/OMPAC	35	Daisy	1.27	13.3
"CBGA 300"	361	Ceramic/full array	25	Daisy	1.27	
"PBGA 300"	313	Plastic/full array/OMPAC	35	Daisy	1.27	13.3
"PBGA 600"	560	Plastic/peripheral/SUPER BGA	42	Daisy	1.27	15.25
"CBGA 600"	625	Ceramic/full array	32.5	Daisy	1.27	
"PBGA 300"	256	Plastic/peripheral	27	Daisy	1.27	10.8
"GW"	256	Plastic/gull wing	30.6	Daisy	0.4	

being carried out and will be presented in a future paper.

2. Test vehicle configuration

Two test vehicle assemblies included plastic and ceramic packages. Both FR-4 and polyimide printed wiring boards (PWBs) with six layers, 0.062 in. thick, were used.

Plastic packages covered the range from OMPAC to SuperBGAs (SBGAs). These were (see also Table 1):

- two peripheral SBGA, 352 and 560 I/O;
- peripheral OMPAC 352 I/O, PBGA 352 and 256 I/O;
- depopulated PBGA 313 I/Os;
- 256 QFP, 0.4 mm pitch

In SBGA, the IC die is directly attached to an oversize copper plate providing better heat dissipation efficiency than standard PBGA. The solder balls for plastic packages were eutectic (63Sn/37Pb).

Ceramic packages with 625 and 361 I/Os were also included in our evaluation. Solder balls for ceramic with 0.035 in. diameters had a high melting temperature (90 Pb/10 Sn). These balls were attached to the ceramic substrate with eutectic solder (63 Sn/37 Pb). At reflow, package side eutectic solder and the PWB side eutectic paste will be reflowed to provide the electro-mechanical interconnects.

Plastic packages had dummy and daisy chains and the daisy chains on PWB were designed so as to be able to monitor critical solder joint regions. Most packages had four daisy chain patterns, 560 I/O had five, and QFP had one.

3. Package dimensional characteristics

Package dimensional characteristics are among the key variables that affect solder joint reliability. Dimensional characteristics of all packages were measured using a 3D laser scanning system for solder ball diameter, package warpage, and coplanarity [2].

4. Test vehicle assembling

Full assembling was implemented after process optimization from the trial test. The following procedures were followed:

1. PWBs were baked at 125°C for 4 h prior to screen printing.
2. Two types of solder pastes were used, an RMA and a water soluble one.
3. Pastes were screen printed and the heights were measured by laser profilometer. Three levels of paste were included in evaluation: standard, high, and low. Stencils were stepped to 50% to accommodate assembling ceramic, plastic, and fine pitch QFP packages in the type 2 test vehicle.
4. A 10 zone convection oven was used for reflowing.
5. The first assembled test vehicle (TV) using an RMA reflow process was visually inspected and X-rayed to check solder joint quality.
6. All assemblies were X-rayed.
7. A reflow profile was also developed for water soluble paste based on the manufacturer's recommendation.

Two test vehicles were assembled:

1. Type 1, ceramic and plastic BGA packages with nearly 300 I/Os.
2. Type 2, ceramic and plastic BGA packages with nearly 600 I/Os. Also utilized was a 256 leaded and a 256 plastic BGA package for evaluating and directly comparing manufacturing robustness and reliability.
3. Assemblies with water soluble flux were cleaned in an Electrovert H500. Those with RMAs were

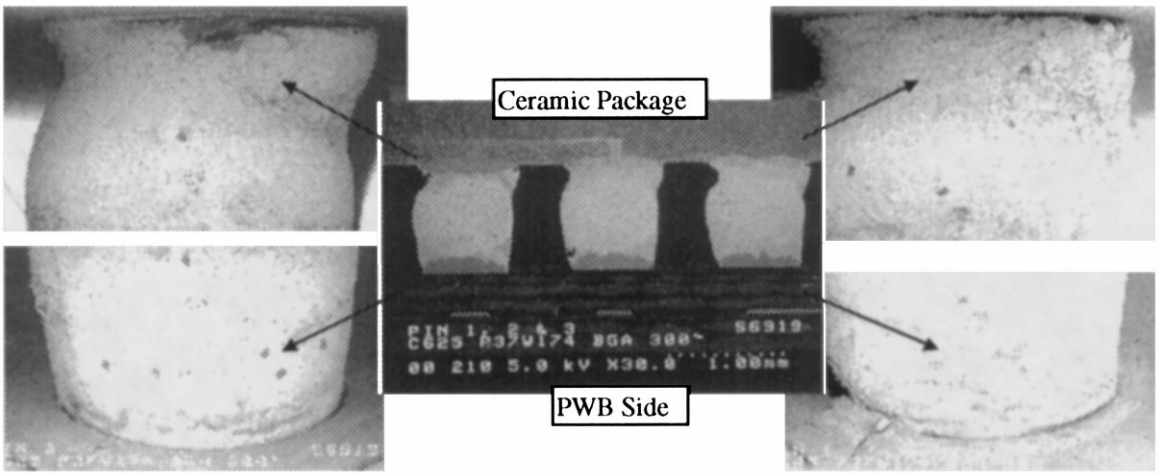

Fig. 1. SEM and cross-section photos for CBGA 625 after 300 cycles, −30°C < - > 100°C.

cleaned used isopropyl alcohol (IPA) and a 5% saponifier.

4. All fine pitch QFPs had to be reworked for bridges.

5. Thermal cycling

The thermal profile and temperature cycling ranges used at the two facilities were significantly different. The JPL cycle (cycle A) ranged from −30 to 100°C and had an increase/decrease heating rate of 2°C–6°C/min and a dwell of about 20 min at hot temperature to assure near complete creeping. The duration of each cycle was 82 min.

Boeing's cycle (cycle B) ranged from −55 to 125°C. It could be also considered a thermal shock since it used a three region chamber: hot, ambient, and cold. Heating and cooling rates were non linear and varied between 10 and 15 °C/min with dwells at extreme temperatures of about 20 min. The total cycle lasted approximately 68 min. BGA test vehicles were continuously monitored through a LabView system at both facilities.

The criteria for an open solder joint specified in IPC-SM-785, Sect. 6.0, were used as guidelines to interpret electrical interruptions. It read in part: "solder joint open circuit is defined as the first interruption of electrical continuity that is confirmed by 9 additional interruptions within an additional 10% of the cyclic life". Generally once the first interruption was observed, there were more than 9 additional interruptions within 10% of the cycle life. In several instances, one or a few early interruptions were not followed by additional interruptions till significantly later stages of cycling. This was found more with plastic packages.

6. Damage monitoring

For conventional SMT solder joints, the pass/fail criteria at JPL relied on visual inspection at 10× to 50× magnifications. For BGA, only edge balls, those not blocked by other components, were visually inspected. A series of single assemblies cut from the test vehicles were used for both visual and SEM inspection to better define visual criteria for acceptance of solder joints as well as monitoring damage progress under different cycling environments.

Fig. 1 shows representative SEM and cross-sectional micrographs for a CBGA 625 after 300 A cycles. Package side eutectic solder joint interfaces, top photos, board interfaces, and bottom photos were included. The left photo is of the corner pin with the maximum DNP (distance to neutral point).

Fig. 2 shows the package interface, top and board interface after 150 B thermal cycles. The left photos are the corner pin and the right photos are for its neighboring pin.

7. Thermal cycling results

7.1. CBGA 625/cycle A condition

Fig. 3 includes cycles to first solder joint failure for CBGA 625 I/Os assemblies on polyimide and FR-4 PWBs with different surface finishes as well as different solder volumes. Results are for those cycled at JPL. The cycles to failure were ranked from low to high and failure distribution percentiles were approximated using median plotting position, $F_i = (i - 0.3)/(n + 0.4)$.

Often, two-parameter Weibull distributions have been used to characterize failure distribution and

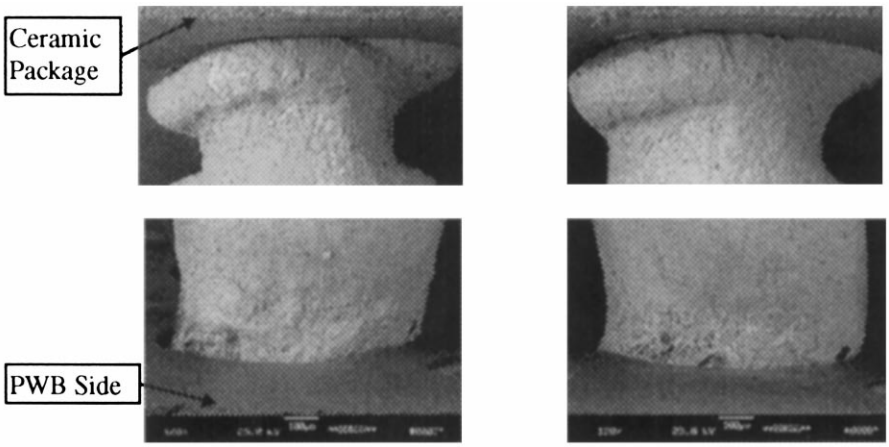

Fig. 2. SEM photos for CBGA 625 after 150 cycles, −55°C < ->125°C.

provide modeling for prediction in the areas of interest. The cycle to failure data in log–log form were fitted to a straight line and the two Weibull parameters were calculated.

For this case, the 2P Weibull scale and shape parameters were 424 and 9.1. The five highest points, four representing those with Ni/Au and one with high solder volume, were excluded in order to get a better fit to data.

7.2. CBGA 625/cycle B condition

Fig. 4 shows the results of the first cycles to failure for CBGA 625 assemblies on FR-4 and polyimide. All assemblies on polyimide showed higher cycles to failure and are shown with different symbols in the plots. One assembly on FR-4 showed unexpectedly very high cycles to failure (398). This data point was not included in the plot.

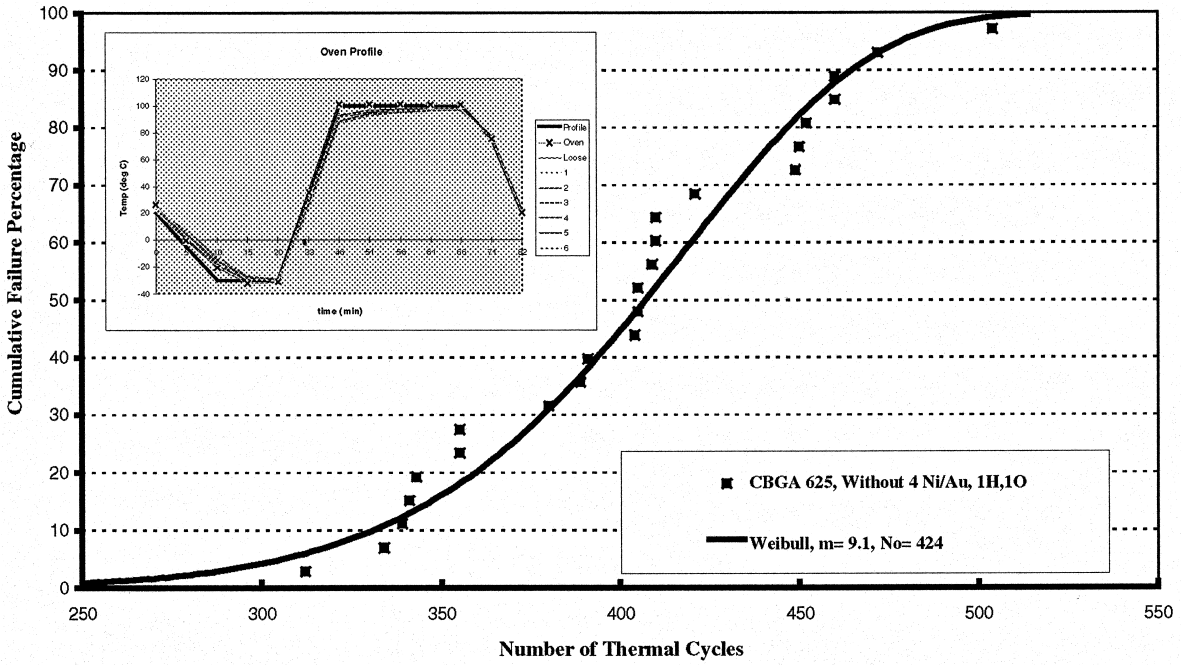

Fig. 3. Cumulative failure distribution and Weibull plot for CBGA 625 I/O assemblies subjected to −30°C < ->100°C with 82 min duration (Cycle A).

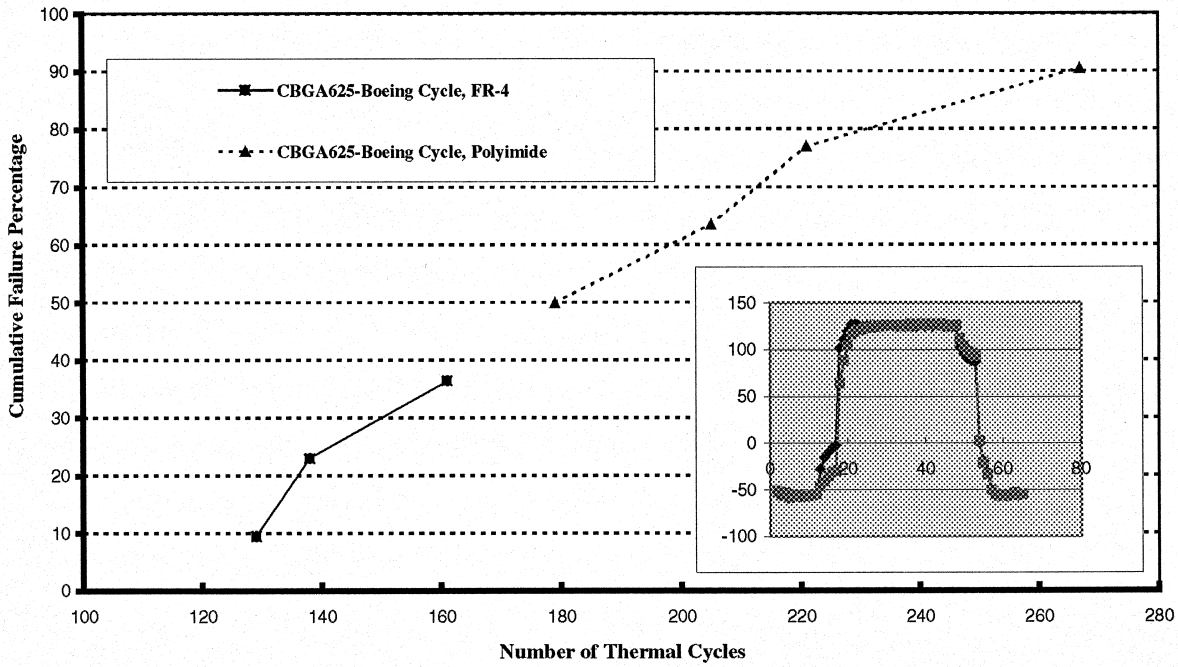

Fig. 4. Cumulative failure distribution for CBGA 625 I/O assemblies subjected to −55°C <-> 125°C (Cycle B) with 68 min duration.

7.3. PBGA 313 and SBGA 352/A and B cycles

Fig. 5 shows cycles to first failure for PBGA 313 and SBGA 352 subjected to the B cycle. The most current PBGA 313 assemblies that failed under the cycle A condition are also included in the plots for comparison. Weibull parameters will be generated when all failure data are gathered.

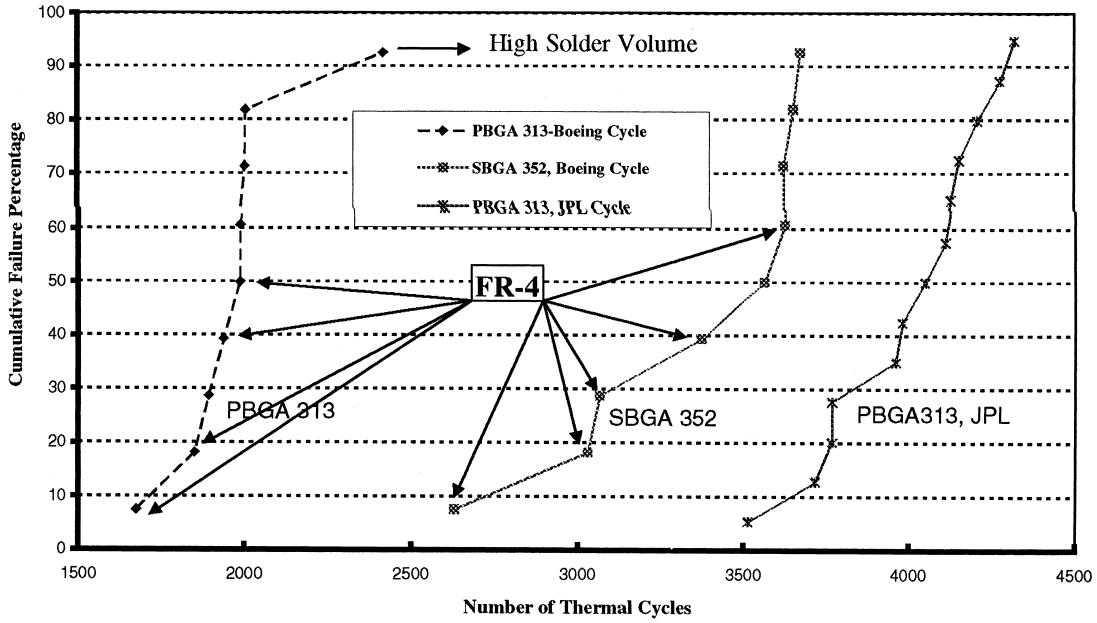

Fig. 5. Cumulative cycling to failure for PBGA 313 assemblies (Cycles A and B) and SBGA 352 (Cycle B).

8. Conclusions

1. As expected, ceramic packages failed much earlier than their plastic counterparts because of their much larger CTE mismatch on FR-4/polyimide boards. Cycles to electrical failure depended on many parameters including cycle temperature range and package size (I/O).
2. Ceramic packages with 625 I/Os were first to show signs of failure among the ceramic (CBGA 361) and plastic packages (SBGA 560, SBGA 352, OMPAC 352, and PBGA 256) when cycled to different temperature ranges.
3. Joint failure mechanisms for assemblies exposed to two cycling ranges were different. Ceramic assemblies cycled in the range of −30°C–100°C (A) showed cracking initially at both interconnections with final separation generally from the board side through eutectic solder. The board side joint showed signs of pin hole formation prior to cracking and complete joint failure. This failure mechanism is similar to those reported in the literature for 0°C–100°C thermal cycles.
4. For −55°C–125°C cycle (B), ceramic packages failed at the package interface with signs of significant creeping, "racheting" effect, and solder grain growth. The board side solder creeping and cracking were much milder.
5. For cycle B, there was a clear distinction between cycles to failure of ceramic 625 I/O on FR-4 and on polyimide, whereas this was not the case with cycle A conditions. Cycles to failure differences could be due to a closer glass transition temperature (T_g) of FR-4 to cycle B's maximum cycling temperature of 125°C.
6. The Coffin–Manson relationships need to be modified to include the effect of higher temperature exposure and heating/cooling rates to be able to project failure of cycle A vehicles for B conditions. Differences in physics of failure mechanisms for CBGAs under the two conditions may invalidate such projections.
7. The PBGAs with 313 I/O, depopulated full arrays, were first among the PBGAs to fail at both cycling ranges. It has been well established that this configuration with solder balls under the die is not optimum from a reliability point of view.
8. Solder volume is generally considered to have a negligible effect on plastic package assembly reliability. One PBGA 313 package that was assembled with high solder paste volume under cycle B exposure showed the highest number of cycles to failure. This will be assessed when data for cycle A become available.
9. The 352 SBGA with no solder balls under the die showed much higher cycles to failure than the PBGA 313 when subjected to cycle B conditions.
10. For cycle B conditions, plastic package assemblies, PBGA 313 and SBGA 352 on polyimide generally failed at a higher number of cycles than those on FR-4.

Acknowledgements

The research described in this publication is being carried out by the Jet Propulsion Laboratory, California Institute of Technology, under a contract with the National Aeronautics and Space Administration.

Special thanks to Sharon Walton at JPL and David Bowen and Kevin Griffith at Boeing for monitoring the environmental testing. We would like to acknowledge the in-kind contributions and cooperative efforts of BGA consortium team members including: P. Barela, K. Bonner, K. Yee, S. Bolin, C. Bodie, JPL; M. Andrews, ITRI; S. Lockwood, M. Simeus, P. Drake, HMSC; I. Sterian, B. Houghton, Celestica; M. Ramkumar, RIT; S. Levine, R. Lecesse, Altron; P. Mescher, AMKOR; W. Goers and J. Mearig, EMPF; M. Cole, A. Trivedi, IBM; and T. Tarter, AMD; F. Schlieper, C. Walquist, Nicolet; R. Dudley, R. Balduf View Engineering. Our deepest appreciation to others who had been or are being contributors to the progress of both programs.

References

[1] Ghaffarian R. Area array technology evaluation for space and military applications. In: The 1996 International Flip Chip Gall Grid Array, TAB and Advanced Packaging Symposium Proceedings, San Jose, February 13–16. Neffs (PA, USA): Semitech, 1996.

[2] Ghaffarian R. CBGA/PBGA package planarity and assembly reliability. In: The 1997 International Flip Chip Ball Grid Array, TAB and Advanced Packaging Symposium Proceedings, San Jose, February 17–19. Neffs (PA, USA): Semitech, 1997.